Envelope Inversion for the Spatiotemporal Distribution of High-Frequency Energy from the M9.0 Tohoku-Oki Earthquake

Asaf Inbal, Jean-Paul Ampuero, Don Helmberger, Seismological Laboratory, California Institute of Technology

1. Introduction

The March 11, 2011 M9.0 Tohoku-Oki earthquake was recorded by dense seismological and geodetical networks deployed in Japan, as well as by a vast number of seismic stations worldwide. These observations allow us to study the properties of the subduction interface with unprecedented accuracy and resolution. In particular, depth-dependent variations of fault behavior, a feature which has long been masked by strong heterogeneities along the fault strike, can now be probed successfully. Back-projection analysis of teleseismic data suggests that coherent high frequency (HF) energy was mainly emitted from deep portions of the megathrust, at the bottom of the rupture zone *(Meng et al.* 2011). Here we study the details of HF energy radiation during the rupture from local observations. Figure 1 summarizes the back-projection results and the corresponding local recordings.
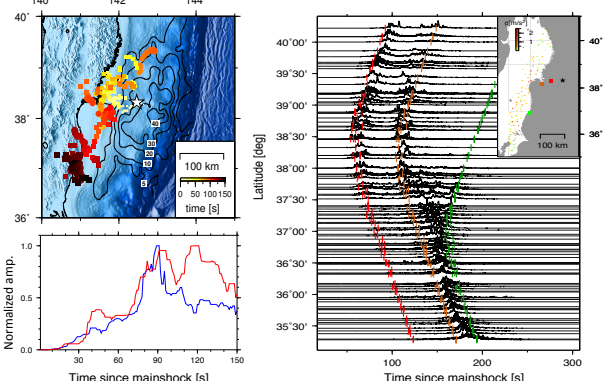
Figure 1. Location map showing the distribution of HF radiators during the rupture (left) and 5-10Hz energy envelopes as a function of latitude (right). White star in upper left panel indicates the hypocentral location. Squares and circles indicate the back-projection results from the US and European arrays, respectively. Symbol size and colors correspond to amplitude and time since the mainshock. Contours are for the coseismic slip distribution of *Simons et al.* (2011). Vertical bars in right panel are for the S-wave arrivals from locations indicated by squares in the inset map. Normalized amplitude as a function of time is shown in bottom left panel for the US (red curve) and European (blue curve) arrays.

2. Methods

We invert waveform envelopes recorded by the KiK-net borehole accelerometers for the spatiotemporal distribution of HF energy radiation. We compute theoretical envelopes for waves travelling in a heterogeneous scattering medium using the method of *Nakahara et al.* (1998). The S-wave energy density envelope at frequency f arriving at station i at time j may be written as:

$$(1) \qquad C_{ij} = S_i(f)G_{ijk}(f)W_k(f),$$

where $S_i(f)$ is the site amplification factor, $G_{ijk}(f)$ is the Green's function for unit energy radiated from cell k, and $W_k(f)$ is the S-wave energy radiated from cell k. We assume constant rupture velocity, and perform a search for rupture velocity and rise time that will minimize the misfit between the observed and calculated envelopes.

Equation (1) assumes that energies are additive, which is true as long as waveforms from adjacent cells are incoherent. To test this assumption we compare envelopes of the sum to the sum of envelopes for two ~M6 events separated by about 15 kilometers. Figure 2 presents the *RMS* of the misfit between the two sums as a function of rupture speed. The envelopes similarity suggests that waveform interference for events separated by distances as small as 15 kilometers is negligible.
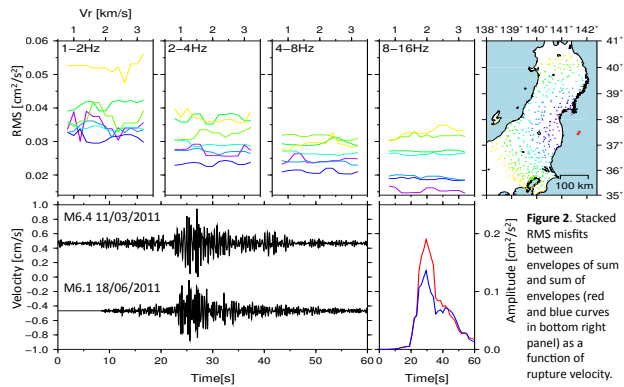
Figure 2. Stacked RMS misfits between envelopes of sum and sum of envelopes (red and blue curves in bottom right panel) as a function of rupture velocity.

2.1 Estimation of site amplification factors

A major difficulty in the inversion procedure is the separation of the source and the station terms. We use the JMA seismicity catalog for the source area and estimate the station terms independently. We adopt the approach of *Shearer et al.* (2006) and iteratively separate the station, source and path terms from the stacked spectra of earthquake clusters occurring along the megathrust. Figure 3 presents the spectral ratio between station FSWH and a reference station as a function of azimuth and incidence angle. Figure 4 presents the spectral ratios for several stations. Note that the amplification factor is correlated with depth to the basement.
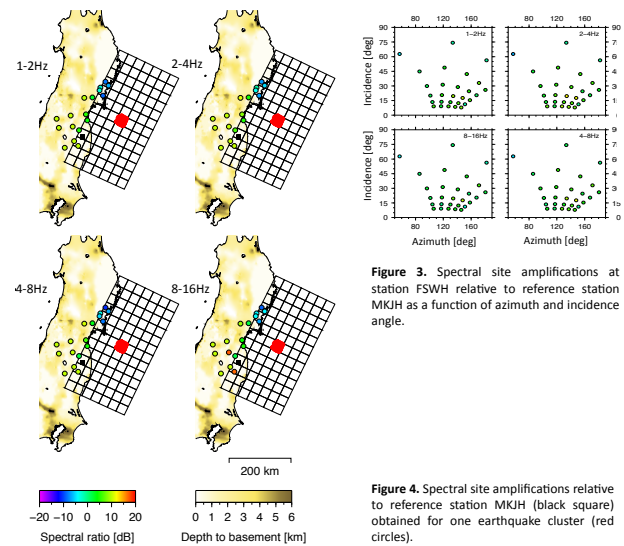

Figure 3. Spectral site amplifications at station FSWH relative to reference station MKJH as a function of azimuth and incidence angle.

Figure 4. Spectral site amplifications relative to reference station MKJH (black square) obtained for one earthquake cluster (red circles).

2.2 Synthetic tests

HF back-projection analysis of *Meng et al.* (2011) suggests that the rupture initially propagated down-dip at speeds of about 1 km/s, and then propagated bilaterally at speeds of about 3 km/s. We perform a synthetic test in which we solve for the HF distribution of an input model with non-constant rupture speed. Figure 5 presents the input model and the inversion results. Note that we are able to resolve the location and amplitude of input HF radiators using an inversion scheme with constant rupture speed.
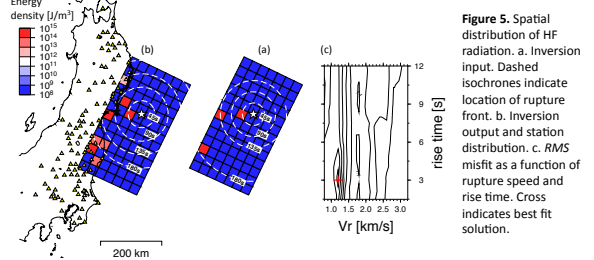
Figure 5. Spatial distribution of HF radiation. a. Inversion input. Dashed isochrones indicate location of rupture front. b. Inversion output and station distribution. c. *RMS* misfit as a function of rupture speed and rise time. Cross indicates best fit solution.

3. Results

Figure 6 presents the output spatial distribution of HF radiators for several frequency bands. Cells up-dip of hypocenter are blurred due to lack of resolution. Note that power from the down-dip edge of the fault increases with frequency. Figure 7 presents the observed and modeled envelopes as a function of time at selected stations.
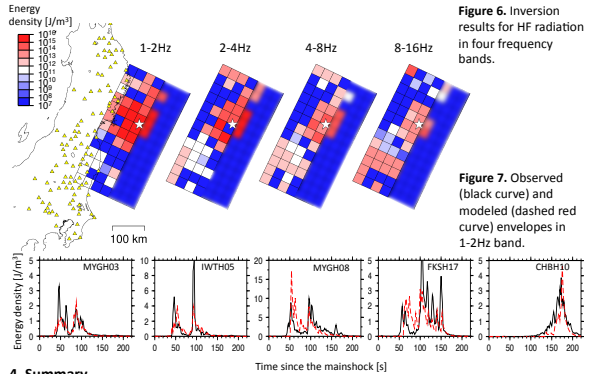
Figure 6. Inversion results for HF radiation in four frequency bands.

Figure 7. Observed (black curve) and modeled (dashed red curve) envelopes in 1-2Hz band.

4. Summary

Spatiotemporal distribution of HF energy during the Tohoku-Oki event originates from the bottom edge of the rupture zone. This result is consistent with teleseismic back-projection analysis. An Inversion scheme with constant rupture velocity is able to capture the prominent features of HF radiation. The power of HF radiation emitted from deeper fault segments increases with frequency.

5. References

Meng L., A. Inbal, and J.-P. Ampuero (2011), A window into the complexity of the dynamic rupture of the 2011 Mw9 Tohoku-Oki earthquake, *Geophys. Res. Lett.*, 38, L00G07, doi:10.1029/2011GL048118

Nakahara H., T. Nishimura, H. Sato, and M. Ohtake (1998), Seismogram envelope inversion for the spatial distribution of high-frequency energy radiation from the earthquake fault: Application to the 1994 far east off Sanriku earthquake, Japan, *J. Geophys. Res.*, 103 (B1), 855-867, doi:10.1029/97JB02676

Shearer P. M., A. A. Prieto, and E. Hauksson (2006), Comprehensive analysis of earthquake source spectra in southern California, *J. Geophys. Res.*, 111 (B06303), doi:10.1029/2005JB003979

Simons M. et al. (2011), The 2011 magnitude 9.0 Tohoku-Oki earthquake: Mosaicking the megathrust from seconds to centuries, *Science*, 332, 1421-1425, doi:10.1126/science.1206731

Digital seismograms and basin depths obtained from Hi-net, KiK-net and NIED (http://www.j-shis.bosai.go.jp)